Journal of Hydroscience and Hydraulic Engineering
Vol. 15, No. 2, December, 1997, 15-30

HORIZONTAL SEPARATION FLOWS IN SHALLOW OPEN CHANNELS WITH SPUR DIKES

By

Fei-Yong CHEN

Water Resources Department, CTI Engineering Company, LTD.

Universal Building, 7-7 Nihonbashi Horidome 1 chome, Chuo-ku, Tokyo 103, Japan

and

Syunsuke IKEDA

Department of Civil Engineering, Tokyo Institute of Technology
12-1 O-okayama 2 chome, Meguro-ku, Tokyo 152, Japan

SYNOPSIS

This paper treats separation flows in shallow open channel with spur dikes by experiment. The formation, development and movement of vortices shed from the tip of spur dikes are studied. The length-scale and the time-scale of horizontal large eddies are found to increase downstream due to merging of vortices. The movement of the reattachment point is also studied. The exchange of momentum and mass between the main flow region and the spur dike region is investigated when two spur dikes are set .

INTRODUCTION

Spur dikes are hydraulic structures constructed mainly to: (1) protect river banks against erosion; (2) train the river along a desired course by attracting, deflecting or repelling the flow in the channel; (3) create a slack flow with objective of silting up the area in the vicinity; and (4) create local scour holes and provide stable, submerged stony substrate for habitat improvement. They are generally used in river engineering. Photo 1 shows a spur dike constructed in Tokachi River, Japan, which is a typical type of modern spur dikes.

The most important aspects to be considered in the design of spur dikes are the layout, plan view, shape length, spacing, crest longitudinal shape, crest elevation, orientation, permeability, construction materials and local scour (Blondeaux and Seminara, 1985). The majority of these aspects are associated with the structures of local turbulent flow, being controlled by the separation flow induced by spur dikes. Hence, flow separation, recirculation and reattachment are the characteristic properties of the turbulent flow in open channels with spur dikes (Fig. 1).

Since the area within and adjacent to the recirculation zones is a major site for sediment deposition, recirculation processes are fundamental in reducing or eliminating bank irregularities and in controlling the morphology of alluvial channels (Leopold et al., 1960; Leeder and Bridges, 1975). Recirculating flow also has been recognized as an important agency for deposition of sands in bedrock channels (Rubin et al., 1990; Schmidt, 1990; Schmidt and Graf, 1990; Andrews, 1991; Nelson, 1991: Schmidt et al., 1993).

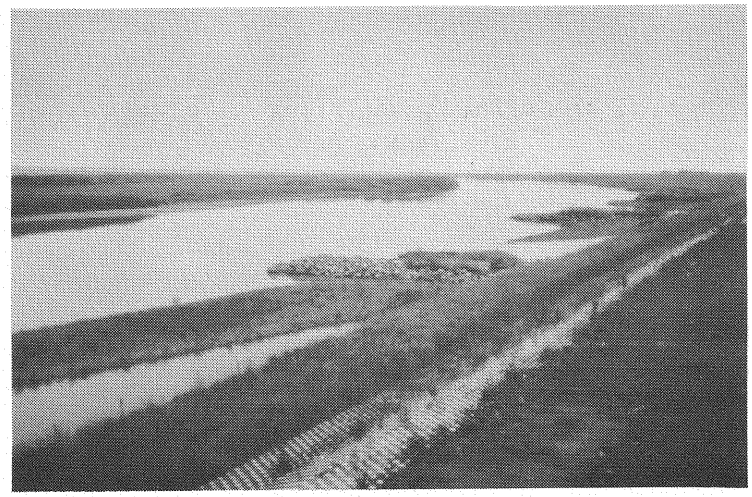

Photo 1 Meander reach of Tokachi River where spur dikes are installed.

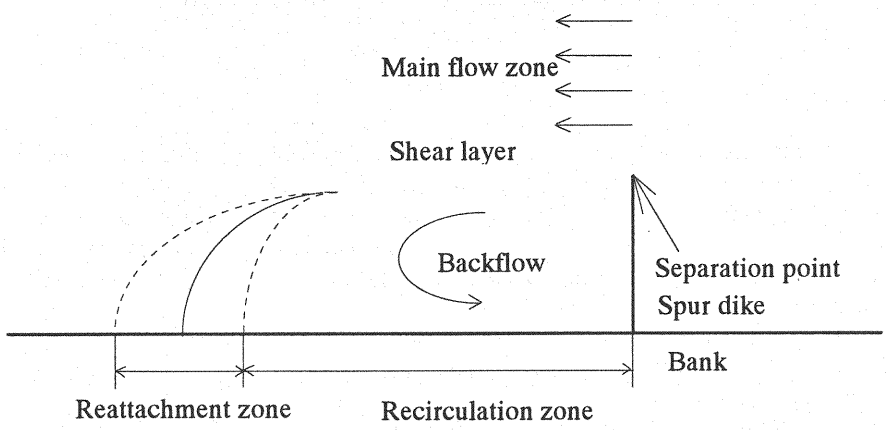

Fig. 1 Plan view of schematized open channel flow with a spur dike.

Schmidt et al. (1993) studied the recirculation zones induced by sand bars along the Colorado River in Grand Canyon, Arizona, and Cataract Canyon, Utah; along the No Return reach of the Salmon River, Idaho; along the Green River in Lodore and Desolation Canyons, Utah; and along small streams in the western United States and New England. They found that recirculation zones were large and persistent, typically occupying one third to one half of the channel width. In the upstream 195 km of Grand Canyon, about 400 lateral eddies exist (Schmidt and Graf, 1990).

Matsuoka (1995) observed flow between two spur dikes in the Chikuma River, Japan. They found that periodic eddies were shed from the tips of spur dikes, and they moved downstream at a speed with the same magnitude of the averaged flow velocity.

Most experimental studies and numerical calculations on separation flows in rivers with spur dikes have been directed to the properties of mean flow (Yeh et al., 1988; Liu et al., 1994; Mayerle et al., 1995). However, as mentioned in the above, the separation flow and the lateral vortices existing in this region are controlling agencies for flow field. In order to understand the structure of turbulent flows induced by spur dikes in shallow open channels, further studies on the lateral eddies and the recirculating flow should be performed. This paper treats the formation, development and

movement of vortices shed from the tip of spur dikes. Mass and momentum exchanges between the main flow region and the recirculation zone are also studied.

EXPERIMENTAL APP.ARATUS AND METHOD

Experiments were conducted at the Hydraulics Laboratory, Department of Civil Engineering, Tokyo Institute of Technology. A tilting flume with 12 m length and 1.2 m×0.3 m cross section (width×height) was used. The flume bottom made of iron was finished with an accuracy of 0.5 mm so as to produce uniform flow. As shown in Fig. 2, a model spur dike which was made of acrylic plate with a size of 30cm×30cm×1cm (length×height×thickness) was set on the left side of flume.

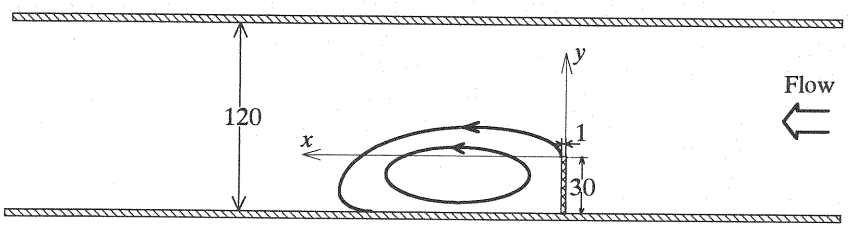

(a) Plan view

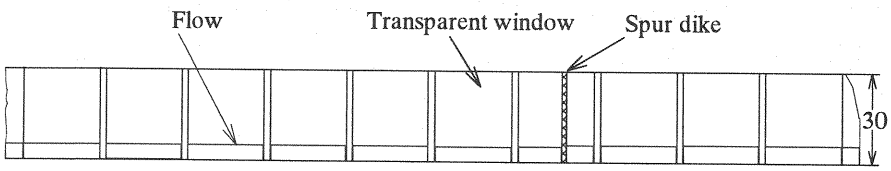

(b) Side view

Fig. 2 Schematic sketch of the experiment (Length unit: cm).

Table 1 Experimental conditions.

CASE	A	B	C	D1	D2	D3	D4	D5	D6	D7
$S_0(10^{-3})$	1.01	0.51	0.72	0.51	0.51	0.51	0.51	0.51	0.51	0.51
H(cm)	4.05	5.20	5.17	5.20	5.20	5.20	5.20	5.20	5.20	5.20
U(cm/s)	31.27	17.36	30.89	17.36	17.36	17.36	17.36	17.36	17.36	17.36
$C_f(10^{-3})$	4.11	8.63	3.79	8.63	8.63	8.63	8.63	8.63	8.63	8.63
u_*(cm/s)	2.01	1.07	1.90	1.07	1.07	1.07	1.07	1.07	1.07	1.07
Fr	0.496	0.243	0.434	0.243	0.243	0.243	0.243	0.243	0.243	0.243
Number of S.D.	1	1	1	2	2	2	2	2	2	2
Distance d between S.D. (cm)				30	60	100	150	200	250	300

Note: S.D.=*Spur Dike.*

Experimental conditions are summarized in Table 1, in which, S_0=bed slope; H = averaged water

depth in a cross section far upstream the spur dikes; U = depth-averaged flow velocity; C_f =friction coefficient of the flume bottom; u_*=the friction velocity evaluated by $\sqrt{gHS_0}$, in which g= gravitational acceleration; Fr= the Froude number. Case A~C were conducted for open channel flows with a single spur dike for different hydraulic conditions. Cases D1~D7 were conducted for flows with two spur dikes. For Case D1~D7, the hydraulic conditions were fixed. However, the distance, d, between two dikes was changed in a range of 30cm~300cm to study the relation between mass and momentum transport rates and the distance d.

The measurements for two components (u, v) of fluid velocity in a horizontal plane were carried out using a miniature electro-magnetic velocimetry (KENEK, VMT2-200-PS08). The size of the probe is 6 mm (diameter). When horizontal organized vortices are migrating downstream, water surface elevation varies with time. The fluctuations of water surface were measured by capacity-type wave gages (KENEK, CHT4-30), for which 512 data were sampled with 0.05 sec. interval for each case.

OPEN CHANNEL FLOW WITH SINGLE SPUR DIKE

Time-Averaged Flow Field

Fig. 3 shows an example of time-averaged flow field measured at a horizontal plane 2.2 cm (about 40% of the water depth) above the flume bottom. Depth-averaged velocities measured at several points suggests that this plane represents well the depth-averaged flow field. Schmidt et al. (1993) subdivided the flow field into four main zones, i.e., main flow zone, shear layer, back flow zone and reattachment zone. In Fig. 3, the former three zones can be observed clearly. From the tip of the spur dike to the right bank of channel, flow velocity is accelerated. This is the main flow zone. The back flow zone is found to locate behind the spur dike. Two circulations can be found in this zone, the center of the larger one locates at about x=180 cm, the other is relatively small, the center of which is seen to exist at about x=25 cm. A velocity difference exists between the main flow zone and the back flow zone, which leads to the existence of a shear layer between the two zones.

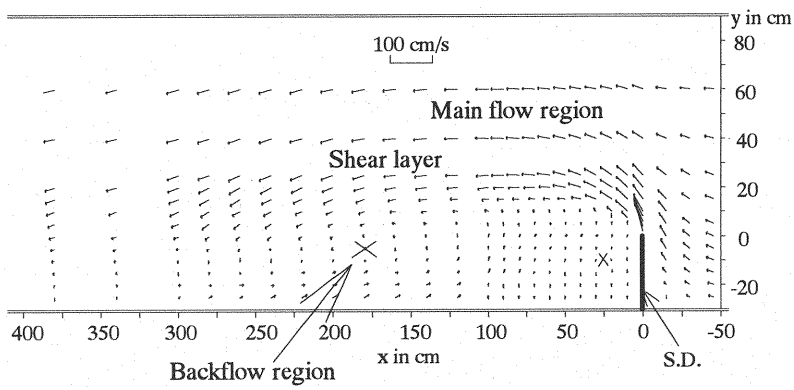

Fig. 3 Time-averaged flow field for Case B (with single spur dike).

Reattachment Point

The flow separated from the tip of the spur dike reattaches to the left bank of the channel at some distance downstream from the spur dike. A simplified drawings of this phenomena is typically shown in Fig. 1 by a time-averaged mean streamline which is impinging on the side wall. However, the instantaneous reattachment point fluctuates back and forth mainly due to the intermittence of eddies in the shear layer and the unstable balance of entrainment and pressure gradient between the

main flow zone and recirculating zone. This zone is termed reattachment zone. The relation between the movement of reattachment point and the migration of large turbulent structures along the shear layer was studied by Schmidt et al. (1993).

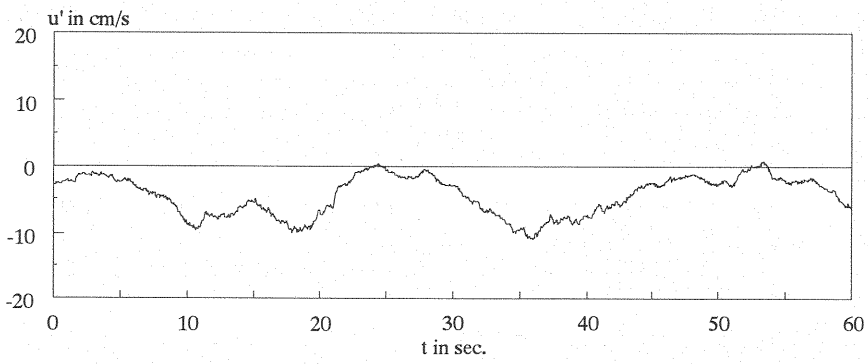

(a) x=340 cm

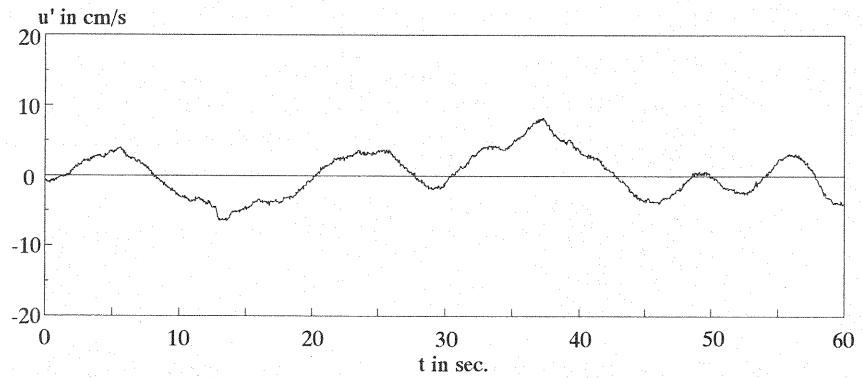

(b) x=420 cm

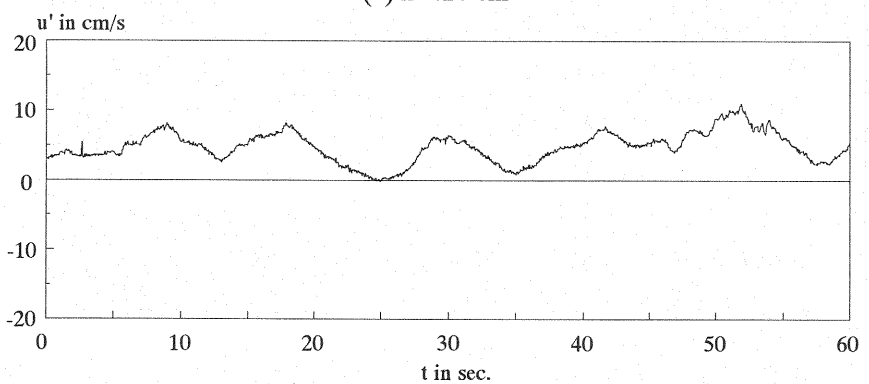

(c) x=520 cm

Fig. 4 Velocity fluctuations at some points in the reattachment zone.

The location of the reattachment point was determined in two ways at the present study. First, visual observation for the time-averaged location of the reattachment point. Second, the velocity fluctuations in the reattachment zone were measured at several longitudinal locations near the side wall by using the electro-magnetic velocimetry. Fig. 4 shows the measured results of velocity fluctuations. Since the separated shear layer impinges on the wall with a large angle at the

reattachment point (see Schmidt et al., 1993), we can regard a point with zero velocity as the temporal reattachment point. In Fig. 4(a), the largest instantaneous velocity is zero, and we can therefore recognize this point as the upstream end of the reattachment zone. In a similar manner, the downstream end of the reattachment zone can be determined by using Fig. 4(c), because the smallest instantaneous velocity at this point is zero. For the velocity fluctuation shown in Fig. 4(b), the time-averaged velocity is found to be zero, suggesting that this is the time-averaged reattachment point.

The longitudinal distance from the spur dike to the time-averaged reattachment point is defined as the length of reattachment zone (Schmidt et al., 1993). It is found that the length of reattachment zone takes an almost constant value for Cases A~C, which was little related with the Froude number within the scope of the present tests. The time-averaged reattachment point locates at x=420 cm, i.e., the reattachment length is 14 times the length of the spur dike. The similar results were found by other researchers (e.g., Schmidt et al., 1993; Mayerle et al., 1995). Schmidt et al. measured the separation zone in Colorado River, and they found that the reattachment length is 13~15 times the length of sand bar.

According to the measurements mentioned in the above, the reattachment zone was found to exist within the range of x=340 cm to x=520 cm. It means that the length of the reattachment zone is 180 cm, i.e., 6 times the length of the spur dike. Schmidt et al. (1993) also found that the location of the reattachment point moved back and forth over distances as large as 4~6 times the length of the sand bar.

Nakagawa et al. (1989) treated a separation from a crest point of sand dune on river bed, and they found that the fluctuation of the reattachment point is related to the structure of large eddies in the shear layer and the period of the fluctuation was about 2 times the period of large eddies. The measurement of velocity fluctuations at the reattachment zone (see Fig. 4) indicates that the period of fluctuation is 13.5 seconds, i.e., about 2 times the period of large eddies there (in the following section, it is observed that the period of large eddies there is about 7 seconds). The reason is not clear.

Water Surface Fluctuation and Mean Water Depth

It has been known that water surface fluctuates when large eddy migrates downstream (Ho and Huerre, 1984; Ikeda et al., 1992). Therefore, the properties of large eddies can be studied by measuring the water surface fluctuation.

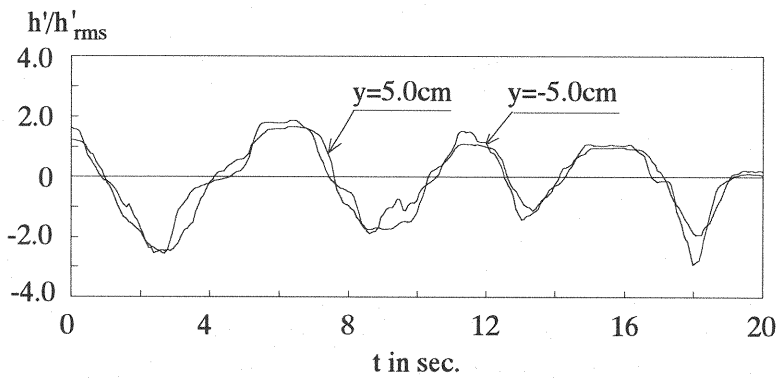

Fig. 5 Time series of water surface fluctuations (Case B, at x=260cm), in which y is the lateral coordinate, taken positive toward the right bank of channel from the tip of the spur dike (see Fig. 2).

Fig. 5 shows the variations of surface elevation at two points in the same cross-section located at

x=260 cm. The lateral locations of the two points are different, but the water surface fluctuations are regularly periodic, and there is not phase difference between them.

The lateral distributions of the root mean square of the water surface fluctuations at several cross sections are depicted in Fig. 6. For every cross section, there is a peak, which suggests that the center of large horizontal vortices locates there. The locations of the peak indicate the time-averaged course of the movement of vortex center.

Fig. 7 shows the variation of the time-averaged water depth along the downstream direction. It suggests that the water depth is considerably changed. It is increased upstream of the spur dike, and decreased downstream of the spur dike. The influence on the water depth induced by the spur dike obviously exists until x=300 cm. The maximum water depth is more than 1.5 times H, and the smallest water depth is about 50% of H.

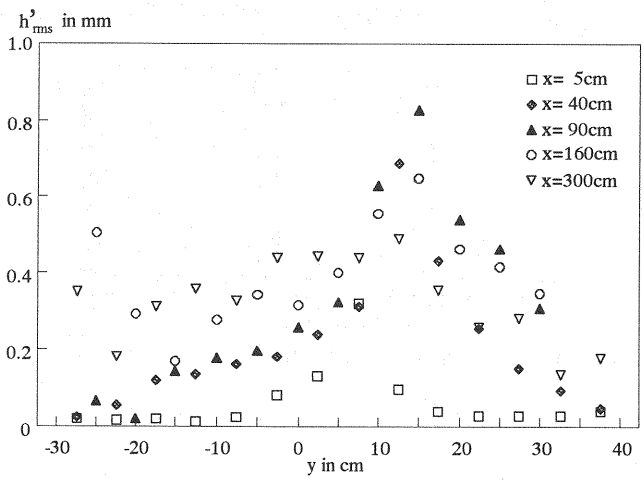

Fig. 6 Lateral distribution of root mean square of water surface fluctuations at several cross-sections (Case B).

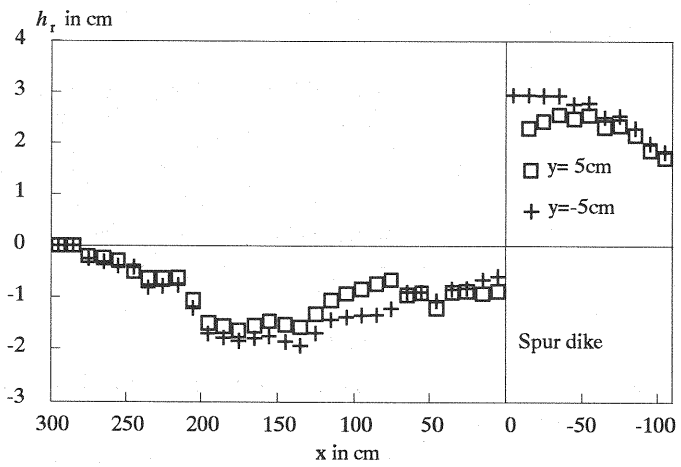

Fig. 7 Spatial variation of relative water depth (Case B), in which $h_r = h - H$.

Horizontal Large Vortices

Horizontal large eddies were found to be shed from the tip of the spur dike with a nearly

constant period (Matsuoka, 1995). In this paper, the period and the moving velocity of large eddies were studied by measuring the water surface fluctuation.

Migration velocity of horizontal large vortices

As shown in Fig. 8, in order to measure the migration velocity of vortices at a point "A", two wave gages were used in tandem. One wave gage was fixed at "A" (the longitudinal distance from the spur dike were defined as x_0), and the location of the another wave gage"B" was changed along the downstream direction within a range of x_r=20~ 40 cm, where x_r is the relative distance between points "A" and "B". The lateral coordinates for these two points were set to be identical, locating at about the center of the vortices.

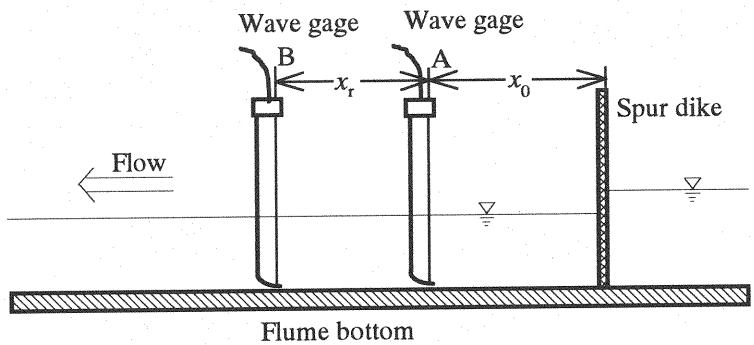

Fig. 8 Arrangement of wave gages for measuring the migration velocity of horizontal large eddies.

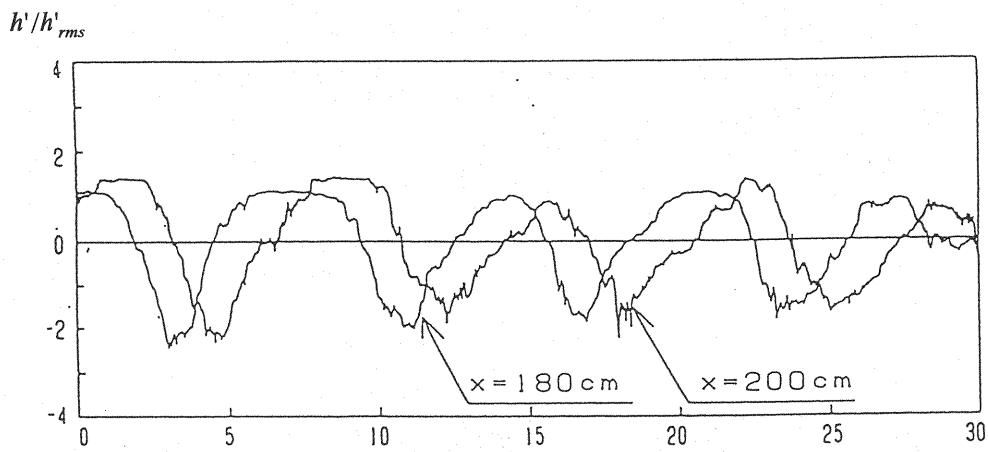

Fig. 9 Illustration of measured water surface fluctuations to test the correlation at two points, x_0 =180 cm, x_r=20 cm (Case B).

An example of time series of water surface fluctuations for two points measured at the same time were shown in Fig. 9. It can be seen that there is a clear phase difference between the two points, which suggests that there is a strong coherency between these two points. The correlation coefficient (denoted by C_a) for each pair of time series of water surface fluctuations was calculated using FFT method. Fig. 10 shows the calculated correlation coefficients of water surface

fluctuations for Case B at x_0 = 30 cm. The lag time when the correlation coefficients takes a peak is considered to be the period that large vortex moves from "A" to "B", which is labeled as t_p. The ratio of x_r to t_p is the migration velocity of vortices. The relation thus obtained is depicted in Fig. 11. A linear relation can be found between x_r and t_p, from which the averaged migration velocity of vortices was found to be 17.60 cm/s for Case B. It is revealed from Fig. 11 that the migration velocity of vortices maintains a constant value everywhere, and this velocity is a little larger than the mean velocity U.

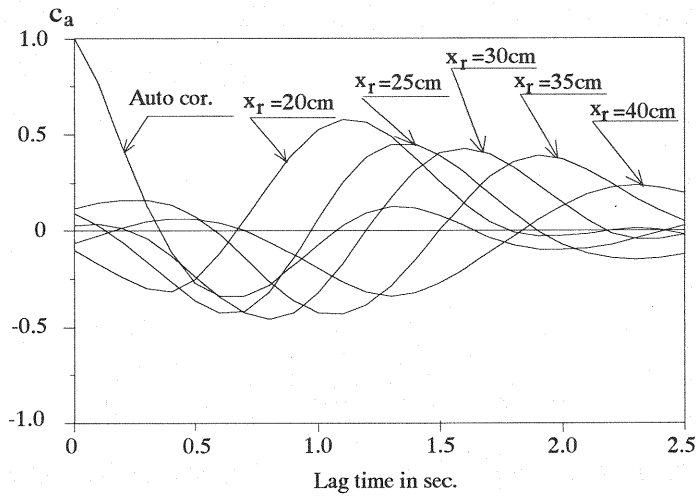

Fig. 10 Variation of the correlation coefficients for water surface fluctuations (Case B, at $x_0 = 30cm$).

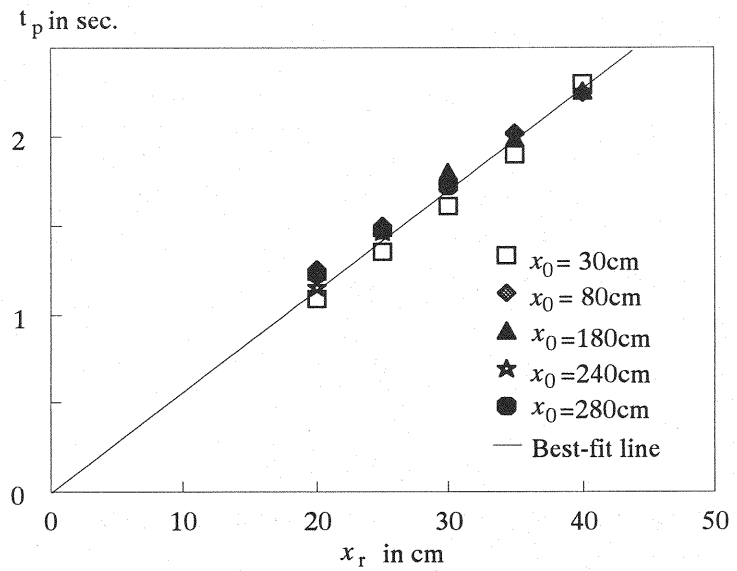

Fig. 11 Determination of the migration velocity of horizontal large vortices (Case B).

Development of horizontal large vortices

As vortices move downstream, they merge with each other by nonlinear interaction. The length

scale of vortices is thus increased downstream (Ho and Huerre, 1984). Since the migrating velocity of vortices is constant everywhere as seen in the above, the time-scale of shed vortices should be increased after merging of vortices. Fig. 12 shows the result, indicating that the time-scale is increased until x=250 cm in this experiment. It indicates that there are frequent merging for relatively small-scale horizontal vortices after being shed from the spur dike until x=250 cm. It should be noted that the time-scale of vortices is found to increase step by step downstream of x=120 cm. The similar result has been found by Ho and Huerre (1984).

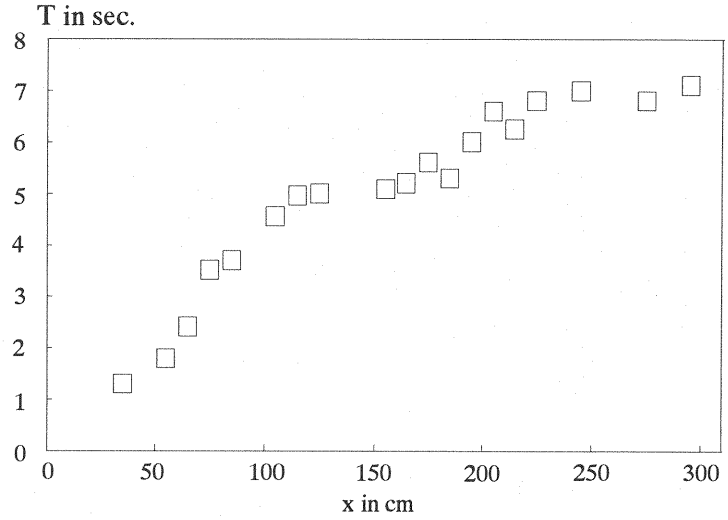

Fig. 12 Development of period of shed large eddies (Case B).

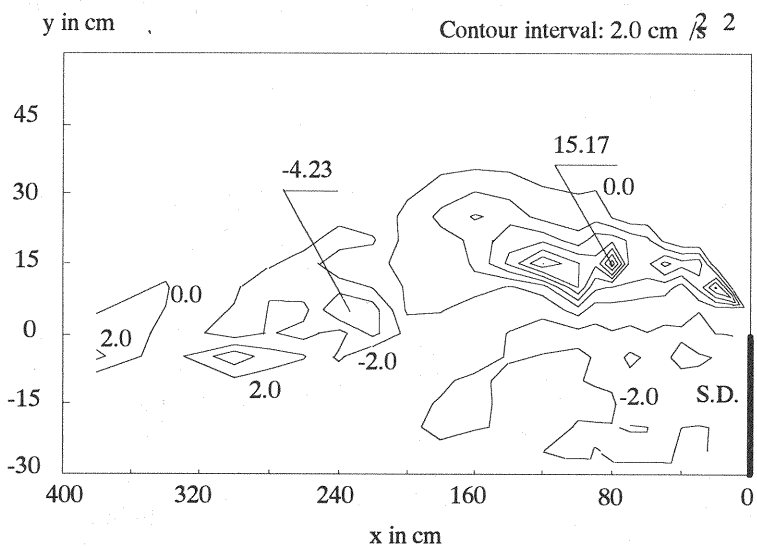

Fig. 13 Contour lines of the Reynolds Stress (Case B).

Reynolds stress

Fig. 13 shows the contour of the Reynolds stress, $-\overline{u'v'}$, for Case B. The location where the Reynolds stress is large is probably the course of movement of vortices. In the downstream zone of the spur dike, negative Reynolds stress is found. At the area downstream from x=200 cm, negative

and positive Reynolds stress contours appear alternately, indicating that a shear layer exists. The peak value of the Reynolds stress is found to locate near the tip of spur dikes, suggesting that the large eddies are generated in the separation flow.

FLOW FIELD WITH TWO SPUR DIKES

Depth-Averaged Flow Field

The depth-averaged flow field for Case D3 is shown in Fig. 14. A recirculating flow can be found between two spur dikes. The reattachment point downstream the second spur dike locates at about x=280cm, suggesting that the length of the reattachment zone from the second spur dike is 6 times the length of the dike. The value is much smaller than that of single spur dike as described previously.

Lateral Velocity Distribution at the Interface of Main Flow Region and Spur Dike Region

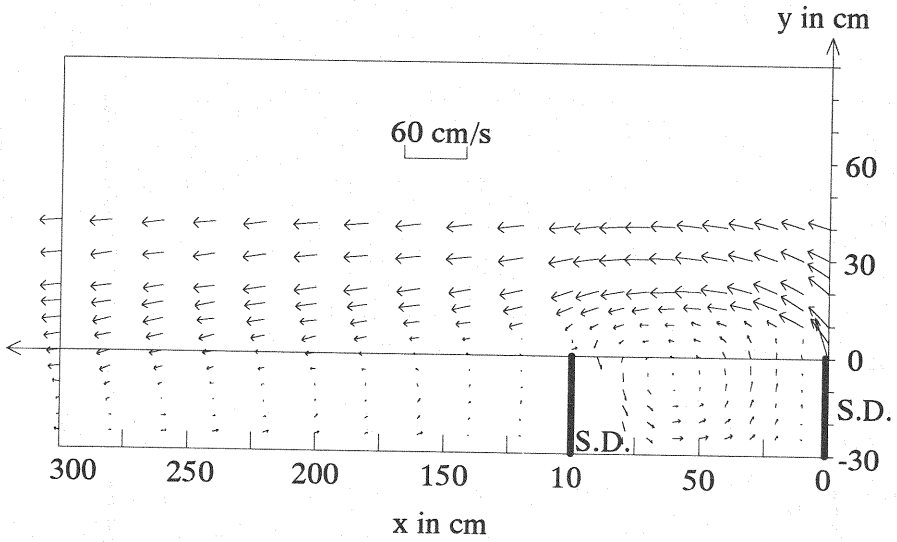

Fig. 14 Time-averaged velocity vector for Case D3 (d=100cm).

The interface connecting the tips of two spur dikes is defined as the boundary between the main flow region and the spur dike region. The lateral velocity at this boundary yields the mass and the momentum exchange between the main flow region and the spur dike region. The lateral time-averaged velocity distributions are shown in Fig. 15, in which l= length of spur dike, d= distance between two spur dikes. From the figure, it is seen that the sign of lateral velocity changes longitudinally, which is associated with the recirculations in the flow field. The number of the changes increases with d, suggesting that for large value of d the number of recirculation is plural. For d=100 cm, the change of the sign of velocity is only one time, but it is 2 and 3 turning times for d=150 cm and 300 cm, respectively. The main factor controlling the turning times, the number that velocity is changing from positive value to negative value, is the ratio of longitudinal scale of recirculation to the distance between two spur dikes.

Fluctuation of Water Surface

When the distance between two spur dikes is changed, the intensity of water surface fluctuation in the spur dike region varies. Fig. 16 shows the variation of the root mean square of water surface fluctuations at a fixed point (x=1.5 cm, y=-15 cm) as d is increased.

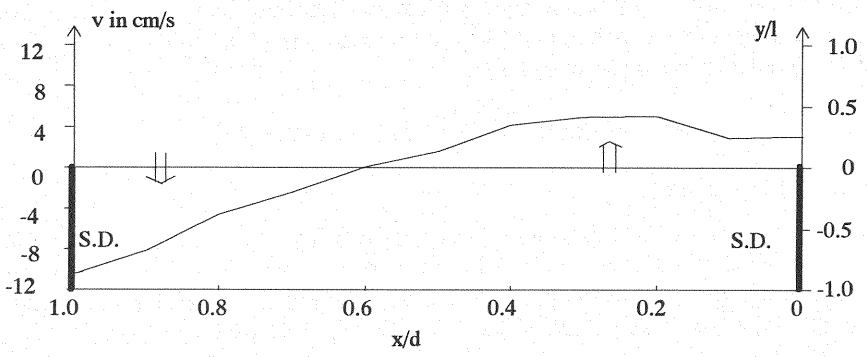

(a) Case D3 (d=100 cm)

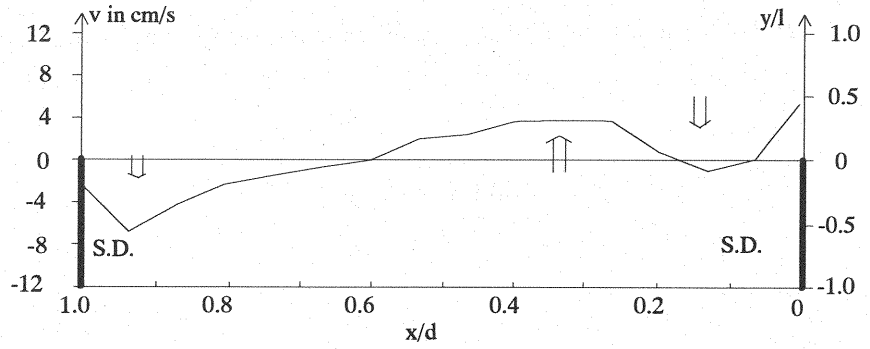

(b) Case D4 (d=150 cm)

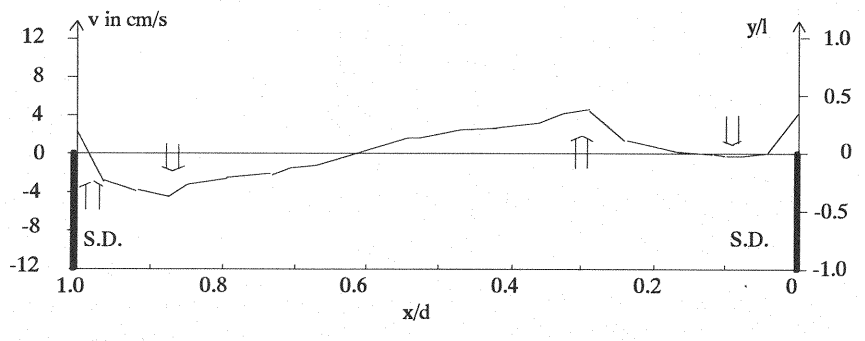

(c) Case D6 (d=250 cm)

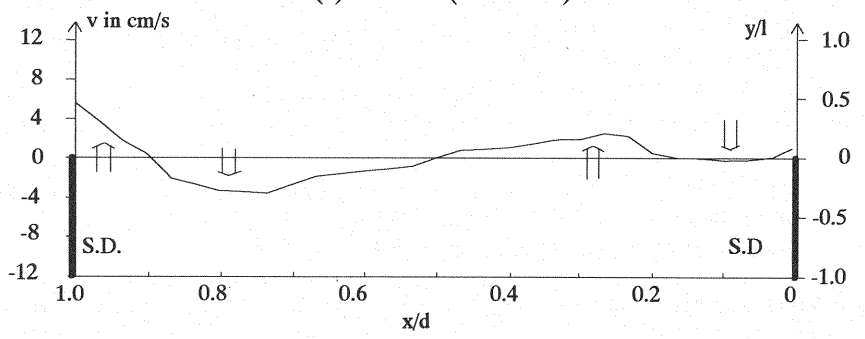

(d) Case D7 (d=300 cm)

Fig. 15 Distributions of time-averaged lateral velocity at the interface of the main flow region and the spur dike region.

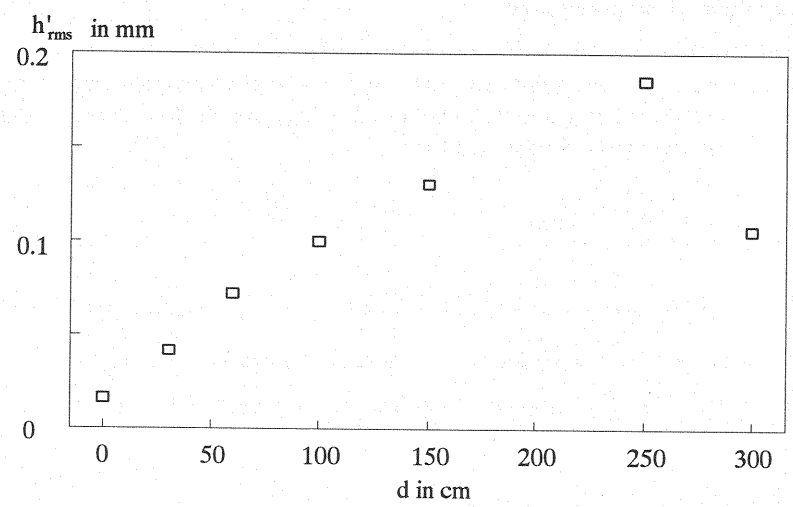

Fig. 16 Variation of the root mean square of water surface fluctuations at a fixed point (x=1.5, y=-15) with the distance between two spur dikes.

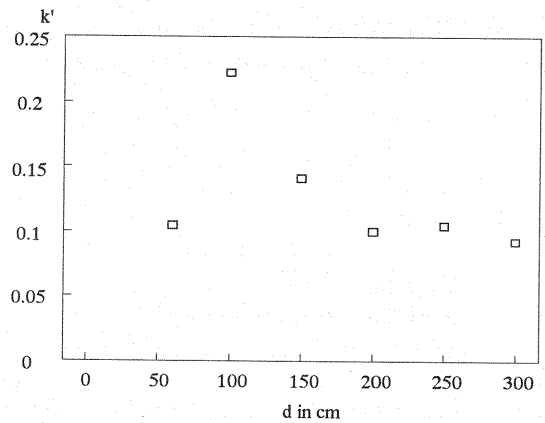

Fig. 17 Relationship of the mass exchange rate with the distance between two spur dikes.

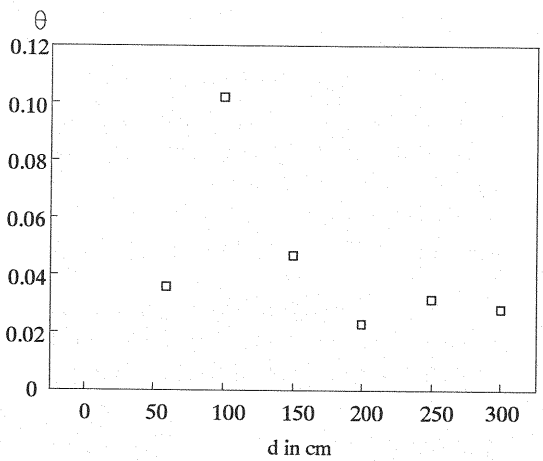

Fig. 18 Relationship of the momentum exchange rate with the distance between two spur dikes.

Mass and Momentum Transport Rates

At the interface of the main flow zone and the spur dike region (y=0 cm), mass and momentum of the flow are exchanged between the main flow region and the spur dike region by the lateral velocity associated with the recirculations. The absolute amount of fluid exchanged through the boundary, Q_t, is estimated by the following relation:

$$Q_t = \int_0^d |v|dx = -2\int_- vdx = 2\int_+ vdx \tag{1}$$

where v= depth-averaged lateral velocity at the boundary (y=0), $\int_+$= integration for the range with positive lateral velocity, and $\int_-$= integration for the range with negative lateral velocity.

In a similarly manner, the total amount of momentum exchanged through the boundary can be calculated using the following relation:

$$P_t = \int_0^d \sqrt{u^2 + v^2}|v|dx \tag{2}$$

where u= depth-averaged streamwise velocity at the boundary (y=0). Let Q_t and P_t be made dimensionless using mean velocity U and the distance, d, which are denoted by k' and θ, respectively. The dimensionless variables, k' and θ, are described as follows, respectively:

$$k' = \frac{1}{Ud}\int_0^d |v|dx \tag{3}$$

$$\theta = \frac{1}{U^2 d}\int_0^d \sqrt{u^2 + v^2}|v|dx \tag{4}$$

The relations of k' and θ with the distance between two spur dikes, d, are shown in Figs. 17 and 18, respectively. The same tendency for k' and θ can be found in the figures. Peaks appear at x=100 cm, and mild peaks appear at x=250 cm for both quantities. The hydraulic parameter which governs the phenomenon is considered to be the ratio of the scale of vortices to the distance, d. Comparing with the Fig. 15, the peak values of k' and θ appear for the cases where the recirculations are stable and well developed.

CONCLUSIONS

In this paper, experimental studies were conducted to investigate the properties of the horizontal vortices, including the merging of the vortices, the migration velocity of the vortices, reattachment of separated flow, etc. The following conclusions are obtained:

(1) The scale of horizontal large vortices increases step by step due to the merging of vortices as they move downstream. Their migration velocity is kept to be constant, which is a little larger than the averaged velocity.

(2) The reattachment point moves periodically back and forth from the time-averaged reattachment point for the case of single spur dike. The period of the fluctuation is about 2 times of the period of the vortices. The reattachment length and the length of the reattachment zone is 14 and 6 times of the length of spur dike, respectively. They are independent of the Froude number within the scope of the present laboratory tests.

(3) The characteristics of flow with two spur dikes is also studied for which the rates of exchange of mass and momentum between the main flow region and the spur dike region are also

studied. The mass and momentum exchange rates were found to be correlated with the ratio of the longitudinal scale of vortices to the distance, d, between two spur dikes. If the recirculating flow, which is closely corrected with horizontal large vortices, between two spur dikes is stable and well-developed, the mass and the momentum exchange rates take peak values.

REFERENCES

Andrews, E.D. : Deposition rate of sand in lateral separation zones, Colorado River (abstract), Eos Transactions, AGU, Vol.72, pp.219, 1991.

Blondeaux, P. and G. Seminara : A unified bar-bend theory of river meanders, Journal of Fluid Mechanics, Vol.112, pp.363-377, 1985.

Ho, C.M. and P. Huerre : Perturbed free shear layers, Annual Review of Fluid Mechanics, Vol..16, pp 365-424, 1984.

Ikeda, S., K. Ohta and H. Hasagawa : Periodic vortices at the boundary of vegetated area along river bank, Proceedings of JSCE, No.443, pp.47-54, 1992 (in Japanese).

Kimura, I., T. Hosoda, Y. Muramoto and R. Yasunaga : Fundamental properties of free surface oscillation in dead zone of open channel flows, Annual Journal of Hydraulic Engineering, JSCE, Vol.39, pp.779-784, 1995 (in Japanese).

Leeder, M.R. and P.H. Bridges : Flow separation in meander bends, Nature, Vol.253, pp.338-339, 1975.

Leopold, L.B. : The rapids and the pools_Grand Canyon, Geological Survey Professional Paper 669, United State Government Printing Office, Washington, pp.131-145, 1969.

Liu, J., A. Tominaga and M. Nagao : Numerical simulation of the flow around the spur dikes with certain configuration and angles with bank, Journal of hydroscience and Hydraulic Engineering, JSCE, Vol..12, No.2, pp.85-100, 1994.

Matsuoka, Y. : Characteristics of large eddies among groins, Annual Journal of Hydraulic Engineering, JSCE, Vol.39, pp.773-778, 1995 (in Japanese).

Mayerle, R., F.M. Toro and S.S.Y. Wang : Verification of a three-dimensional numerical model simulation of the flow in the vicinity of spur dikes, Journal of Hydraulic Research, IAHR, Vol.33, No.2, 1995.

Nakagawa, H., I.Nezu, T.Matsumoto and F.Kanagawa : Turbulent structure and Coherent vortex over the dune bed in open channel flows, Annual Journal of Hydraulic Engineering, JSCE, Vol.33, pp. 475-480, 1989 (in Japanese).

Nelson, J.M. : Experimental and theoretical investigation of lateral separation eddies (abstract)", Eos Transactions, AGU, Vol.72, pp.218-219, 1991.

Rubin, D.M., J.C. Schmidt and J.N. Moore : Origin, structure, and evolution of a reattachment bar, Colorado River, Grand Canyon, Arizona, Journal of Sedimentary Petrology, Vol.60, pp.982-991, 1990.

Schmidt, J.C. : Recirculating flow and sedimentation in the Colorado River in Grand Canyon, Arizona, the Journal of Geology, AGU, Vol.98, pp.709-724, 1990.

Schmidt, J.C. and J.B. Graf : Agradation and degradation of alluvial sand deposits, 1965 to 1986, Colorado River, Grand Canyon National Park, Arizona, Geological Survey Professional Paper 1493, United State Government Printing Office, Washington, 1990.

Schmidt, J.C., D.M. Rubin and H. Ikeda : Flume simulation of recirculating flow and sedimentation, Water Resources Research, AGU, Vol.29, pp.2925-2939, 1993.

Simpson, R.L. : Turbulent boundary-layer separation, Annual Review of Fluid Mechanics, Vol.21, pp. 205-234, 1989.

Yeh, H.H., W. Chu and O. Dahlberg : Numerical modeling of separation eddies in shallow water, Water Resources Research, AGU, Vol.24, pp.607-614, 1988.

APPENDIX-NOTATIONS

The following symbols are used in this paper:

B = channel width;

c = migration velocity of large eddies;

c_a = correlation coefficient;

C_f = bottom friction coefficient;

d = interval between two spur dikes;

g = gravitational acceleration;

h = water depth;

h' = water surface fluctuation;

h'_{rms} = root mean square of water surface fluctuation;

H = mean water depth;

k' = dimensionless mass exchange rate;

l = length of spur dike;

P_t = total amount of momentum exchanged between the main flow region and the spur dike region per unit time;

Q_t = total amount of mass exchanged between the main flow region and the spur dike region per unit time;

S_0 = longitudinal channel bed slope;

t = time;

t_p = lag time for large eddies migrating form one point to another point downstream;

u = local longitudinal component of time-averaged velocity;

u' = fluctuation of longitudinal velocity component;

U = undisturbed mean streamwise velocity;

v = transverse time-averaged velocity;

v' = fluctuation of transverse velocity component;

x_0 = longitudinal location for Wave gage "A" (see Fig. 7);

x_r = longitudinal distance between two wave gages;

x, y, z = longitudinal, transverse, and vertical coordinate, respectively; and

θ = dimensionless momentum exchange rate.

(Received March 5, 1997; revised October 6, 1997)